Journal of Alloys and Compounds 321 (2001) 27–34
www.elsevier.com/locate/jallcom

Structure and magnetism of R_5Bi_3 (R=Tb, Dy, Ho, Er) and Tb_4Bi_3

M. Drzyzga*, J. Szade

Institute of Physics, University of Silesia, Uniwersytecka 4, 40-007 Katowice, Poland

Received 29 November 2000; accepted 12 February 2001

Abstract

The physical properties of the rare earth bismuthides R_5Bi_3 (R=Tb, Dy, Ho, Er) and Tb_4Bi_3 were investigated for the first time. The R_5Bi_3 compounds have been found to crystallise in the orthorhombic structure of the Y_5Bi_3-type whereas Tb_4Bi_3 forms the cubic anti-P_4Th_3 structure. The temperature dependence of the DC and AC magnetic susceptibility and the electrical resistivity have been measured. Tb_4Bi_3 orders ferromagnetically at 190 K whereas R_5Bi_3 show a complex form of magnetic ordering at lower temperatures.

Keywords: Rare earth compounds; Crystal structure; Electronic transport; Magnetic measurements

1. Introduction

Compounds of rare earth with non-magnetic metals have been intensively investigated over many years. However only a few systematic studies of rare earth compounds with bismuth have been performed so far. The single crystals of Gd monopnictides, including GdBi, have been investigated with many techniques including X-ray photoemission [1–3]. Our earlier paper reports on the magnetic properties and electronic structure of polycrystalline Gd_4Bi_3 and Gd_5Bi_3 [4] indicating to the relations between these properties. The existing phase diagrams for the systems of rare earth and bismuth show that compounds with the 4:3 stoichiometry exist only for the light rare earths, Gd and Tb, whereas compounds of the 5:3 type are present in the whole rare earth series [5,6]. Yoshihara et al. [7] described two various crystal structures for the composition close to R_5Bi_3 where R is Gd, Tb, Dy, Ho and Er. No studies of the physical properties were described for this group of compounds up to now.

In the present work we obtained the polycrystalline samples of Tb_4Bi_3 and R_5Bi_3 (for R=Tb, Dy, Ho and Er) and studied their structure, magnetism and electrical resistivity.

2. Experimental

The preparation of the samples was similar to the procedure described in our earlier paper on Gd-Bi compounds. The high vapour pressure of Bi and the high temperatures of compound formation make the sample preparation complicated. The polycrystalline samples of R_5Bi_3 (R=Tb, Dy, Ho, Er) and Tb_4Bi_3 were obtained using induction melting in a two-step process. In the first step the pieces of R (R=Tb, Dy, Ho, Er) (99.9%) and Bi (99.999%) were melted together using a levitation coil described elsewhere [8]. The starting weight of Bi was taken to exceed the stoichiometric one by 10% to balance the evaporated amount of this metal. Melting was performed in an argon atmosphere at an overpressure of about 400 mbar. The obtained porous mixture was then remelted several times. During that process the weight loss was 7–8 wt.% and the final weight of a sample was close to the assumed one. Samples of R_5Bi_3 (R=Tb, Dy, Ho, Er) were annealed for 1 week at 1000°C, in vacuum. The weight loss during the annealing was negligible.

The DC magnetic susceptibility measurements were performed using the Faraday method in the temperature range 4.2–700 K, under an atmosphere of helium. The AC magnetic susceptibility was measured in the range 4.2–300 K, using a magnetic field with a frequency of 700 Hz and an amplitude of about 0.5 Oe.

---

*Corresponding author. Tel.: +48-32-587-978; fax: +48-32-588-431.
E-mail address: szade@us.edu.pl (M. Drzyzga).

0925-8388/01/$ – see front matter
PII: S0925-8388(01)01009-X

The electrical resistivity was measured by the van der Pauw method in the temperature range 4.2–300 K.

3. Results and discussion

3.1. Structural study

The survey of the rare earth–bismuth phase diagrams [5] shows that both R_5Bi_3 and Tb_4Bi_3 are formed by a peritectic reaction. We tried to obtain compounds with a composition 4:3 for all heavy rare earths but only for Tb a sample of a reasonable quality was formed. Its crystal structure was the same as for Gd_4Bi_3 – cubic of the anti-P_4Th_3 type. The lattice constant of the cubic structure agrees with the previous data (9.3215 Å) [7]. Similarly to the Gd_4Bi_3, a small amount of the hexagonal Tb_5Bi_3 phase was present in the diffraction pattern of Tb_4Bi_3. All the X-ray diffraction spectra exhibited some peaks due to metallic Bi and for some of them a small amount of the cubic RBi phase was detected.

We have investigated the samples of all compounds with a scanning electron microscope (SEM) and Auger electron spectroscopy (AES). The samples which were fractured in the ultra high vacuum revealed uniform composition. For the samples with Tb we have observed some spherical parts which were attributed to metallic Bi using the AES analysis (Fig. 1). The size of these precipitations was about 1–5 μm. The presence of metallic Bi in the inter-grain boundaries may explain the common feature of the X-ray diffraction patterns from most samples, i.e. broad peaks which could be attributed to Bi. During the powdering process a very small amount of the soft Bi metal may cover the grains of a compound with a thin Bi film.

The Rietveld analysis of the patterns was performed using the FULLPROF program taking as a starting point the parameters from the paper by Yoshihara et al. [7] or Wang et al. [9]. The diffraction pattern of all R_5Bi_3 compounds was consistent with the orthorhombic structure of the Y_5Bi_3-type (space group *Pnma*), reported earlier for the $R_{5+x}Bi_3$ compounds by Yoshihara et al. [7] and for Ho_5Bi_3 by Abulhajev [6]. The detailed analysis of this structure has been done for Y_5Bi_3 by Wang et al. [9]. The unit cell of the structure is shown in Fig. 2. It contains four molecules, there are four in-equivalent positions of R atoms and two of Bi. The lattice constants derived from the patterns are slightly smaller than the ones reported earlier [7] (Table 1). The lanthanide contraction is well reproduced in the variation of the unit cell volume (Fig. 3). Table 2 shows the derived coordinates of particular atoms in a unit cell including the data for Gd_5Bi_3 which have not been published in the previous paper. The coordinates of atoms do not vary much from one to another compound.

3.2. Magnetic susceptibility and electrical resistivity

Tb_4Bi_3 appears to order ferromagnetically at relatively high temperature, i.e. 190 K. The magnetic transition is

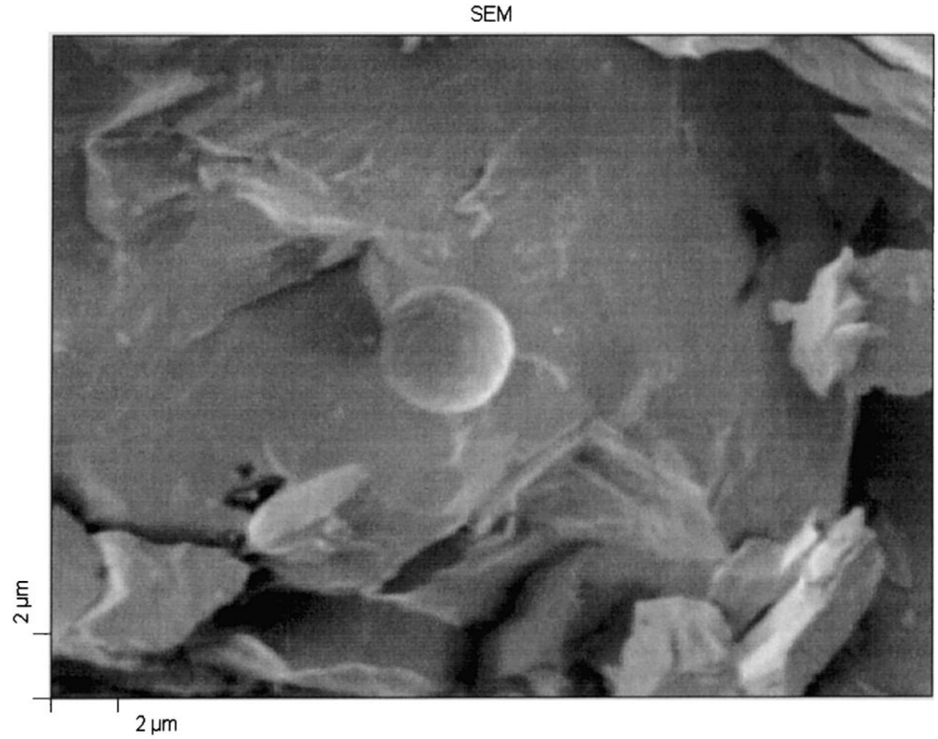

Fig. 1. Scanning electron microscopy (SEM) image of a fractured Tb_5Bi_3 sample with a spherical precipitation of Bi form.

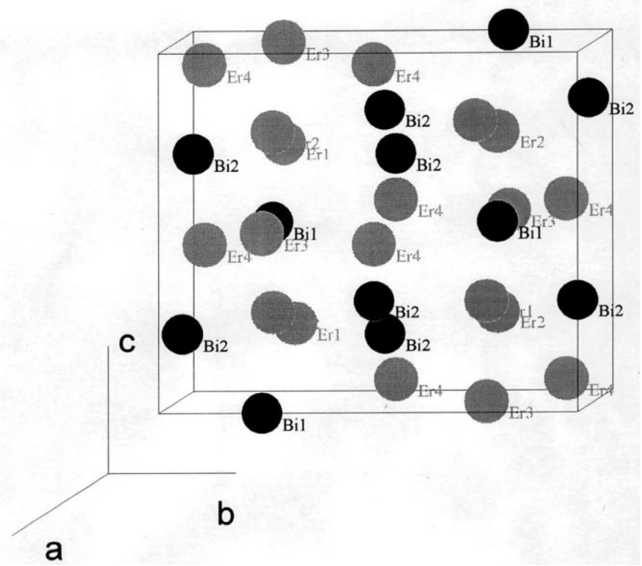

Fig. 2. Unit cell of Er_5Bi_3-characteristic for all R_5Bi_3 compounds. The positions of atoms are indicated.

Table 1
The lattice constants of R_5Bi_3 (R=Tb, Dy, Ho, Er). The error of the refinement may be estimated as 0.001 Å

Compounds	*a* (Å)	*b* (Å)	*c* (Å)
Gd_5Bi_3	8.226	9.540	12.085
Tb_5Bi_3	8.170	9.487	11.968
Dy_5Bi_3	8.155	9.432	11.934
Ho_5Bi_3	8.128	9.385	11.874
Er_5Bi_3	8.090	9.349	11.806

manifested as a step like increase in the DC susceptibility, but the AC one shows a sharp peak, which is unusual for a simple ferromagnetic transition (Figs. 4 and 5). An additional step in the magnetisation is visible at about 100 K, which correlates with a small cusp in the AC susceptibility. The imaginary part of the AC susceptibility shows also a slight bump at that temperature besides of the small

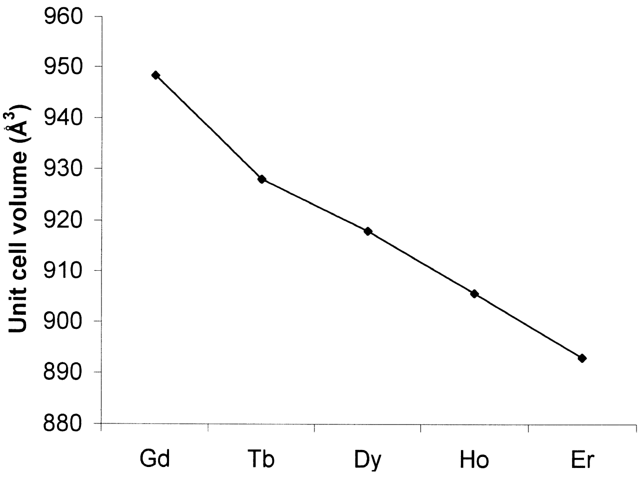

Fig. 3. Unit cell volume of R_5Bi_3 compounds.

Table 2
Fractional positional coordinates for R_5Bi_3 (R=Tb, Dy, Ho, Er)

Atom position	Type of position	*x*/*a*	*y*/*b*	*z*/*c*
Gd_5Bi_3				
Bi1	8d	0.065(1)	0.0056(9)	0.172(4)
Bi2	4c	0.092(1)	0.25	0.454(2)
Gd1	4c	0.4819(1)	0.25	0.455(2)
Gd2	4c	0.346(1)	0.25	0.215(1)
Gd3	8d	0.200(3)	0.559(2)	0.45(1)
Gd4	4c	0.164(3)	0.25	0.7126
Tb_5Bi_3				
Bi1	8d	0.0677(1)	0.0010(7)	0.1716(4)
Bi2	4c	0.0869(1)	0.25	0.4546(2)
Tb1	4c	0.4645(4)	0.25	0.4694(4)
Tb2	4c	0.345(2)	0.25	0.2117(1)
Tb3	8d	0.1982(1)	0.5577(5)	0.4574(1)
Tb4	4c	0.174(1)	0.25	0.7123(2)
Dy_5Bi_3				
Bi1	8d	0.0703(2)	0.0010(6)	0.1711(4)
Bi2	4c	0.0817(1)	0.25	0.4555(3)
Dy1	4c	0.447(1)	0.25	0.4837(2)
Dy2	4c	0.3441(4)	0.25	0.2084(5)
Dy3	8d	0.1928(4)	0.5564(1)	0.4647(4)
Dy4	4c	0.1839(7)	0.25	0.7126
Ho_5Bi_3				
Bi1	8d	0.0680(6)	0.001(1)	0.1734(7)
Bi2	4c	0.0695(3)	0.25	0.4477(2)
Ho1	4c	0.4803(1)	0.25	0.4932(8)
Ho2	4c	0.374(2)	0.25	0.179(1)
Ho3	8d	0.1983(2)	0.5566(5)	0.443(2)
Ho4	4c	0.1654(5)	0.25	0.71260
Er_5Bi_3				
Bi1	8d	0.0695(2)	0.001(1)	0.1667(2)
Bi2	4c	0.0933(2)	0.25	0.4495(4)
Er1	4c	0.4794(4)	0.25	0.4730(4)
Er2	4c	0.3320(2)	0.25	0.2464(4)
Er3	8d	0.1847(7)	0.5646(8)	0.4477(2)
Er4	4c	0.1701(2)	0.25	0.71260

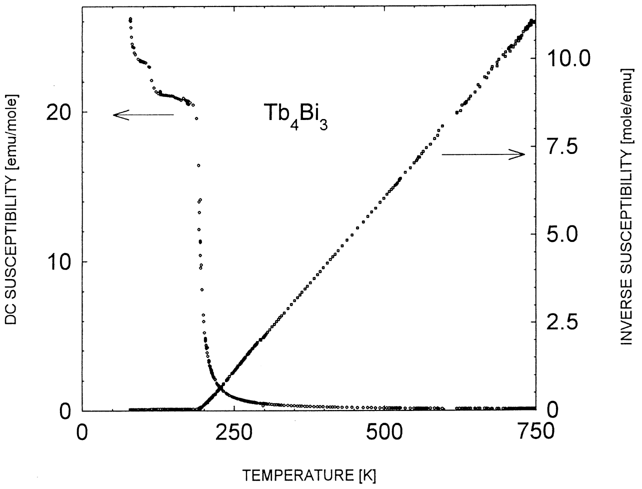

Fig. 4. Temperature dependence of magnetic susceptibility for Tb_4Bi_3.

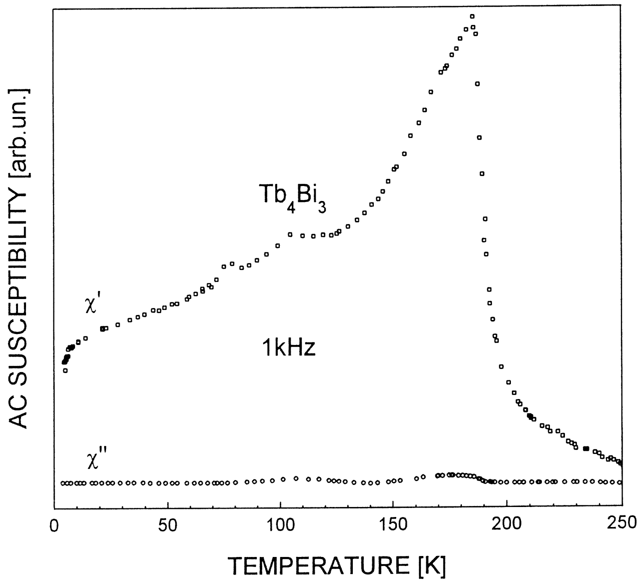

Fig. 5. AC magnetic susceptibility vs. temperature for Tb_4Bi_3.

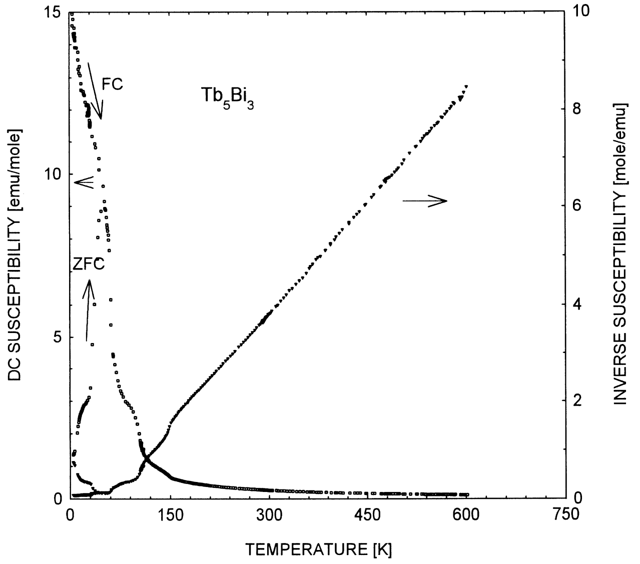

Fig. 7. Temperature dependence of magnetic susceptibility for Tb_5Bi_3. FC means cooling in the field of 854 Oe. ZFC, zero field cooling.

step at 190 K. One may suppose that the main ordering, which starts at 190 K, is not a simple ferromagnetic one and a spin reorientation takes place below T_C. The electrical resistivity exhibits a transition at about 180 K which divides the $\rho(T)$ run into two regions: one of the constant resistivity above T_C and the second one, which is characterised mainly by a negative curvature (Fig. 6). The resistivity still decreases when approaching 4.2 K. The paramagnetic Curie temperature corresponds very well to T_C and the effective moment is higher by about 0.3 μ_B than the theoretical value (Table 3).

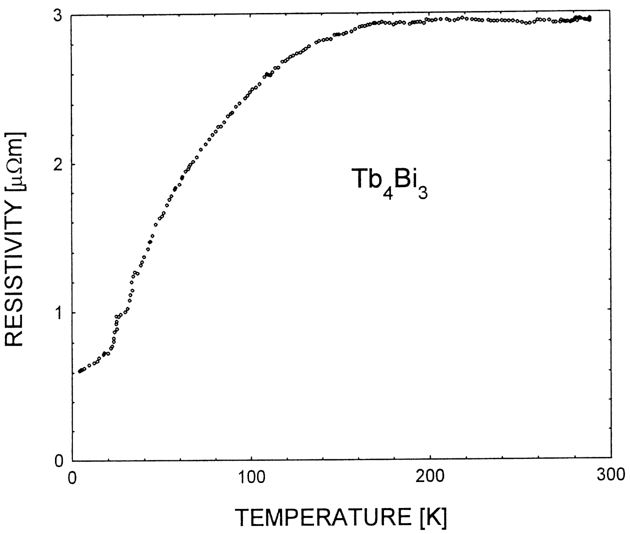

Fig. 6. Electrical resistivity in function of temperature for Tb_4Bi_3.

The properties of Tb_4Bi_3 can be compared to the ones described earlier for the isostructural Gd_4Bi_3 [4]. The Gd compound is a ferromagnet with T_c=335 K, which is a very high value for a compound with a non-magnetic element, and it also shows a peak in the AC susceptibility below T_C. The resisitivity of Tb_4Bi_3 is higher than that of Gd_4Bi_3 but the character of the temperature dependence is similar. Despite of the fact that Tb_4Bi_3 is a compound which limits the series of this composition within rare earths, its crystal structure seems to be more stable than that of Gd_4Bi_3 which exhibits structural changes when heated above the room temperature [4].

Similarly to the previously studied Gd_5Bi_3 [4], the magnetic ordering in other R_5Bi_3 takes place at relatively low temperatures and shows a complex behaviour. The Curie–Weiss behaviour is observed in a large temperature

Table 3
Magnetic properties of R_5Bi_3 (R=Tb, Dy, Ho, Er) and Tb_4Bi_3

Compound	$g_J\,[J(J+1)]^{1/2}$ [μ_B]	Effective magnetic moment μ_{eff} [μ_B]	Paramagnetic Curie temperature Θ_p [K]
Tb_4Bi_3	9.72	10.06	192
Gd_5Bi_3	7.94	8.43	120
Tb_5Bi_3	9.72	10.31	52
Dy_5Bi_3	10.64	10.18	30
Ho_5Bi_3	10.6	10.73	11
Er_5Bi_3	9.58	9.42	7

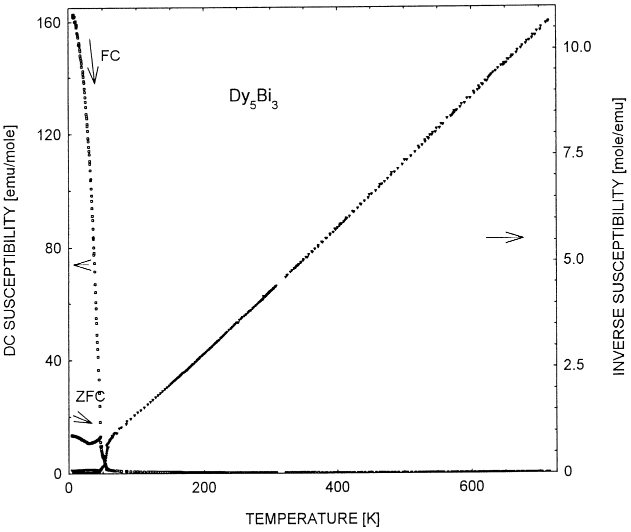

Fig. 8. Temperature dependence of magnetic susceptibility for Dy_5Bi_3. FC means cooling in the field of 570 Oe. ZFC, zero field cooling.

range 200–700 K. The positive values of the paramagnetic Curie temperatures were obtained for all compounds indicating to a dominant ferromagnetic interaction. The effective magnetic moment is higher than a theoretical one for the Tb compound and is close to the theoretical values for other compounds (Table 3). The susceptibility of some compounds shows some anomalies at temperatures higher than the main magnetic transition (Figs. 7–10). They do not seem to be related to the presence of an additional RBi phase as GdBi exhibits an antiferromagnetic ordering at very low temperature of 25.8 K [2].

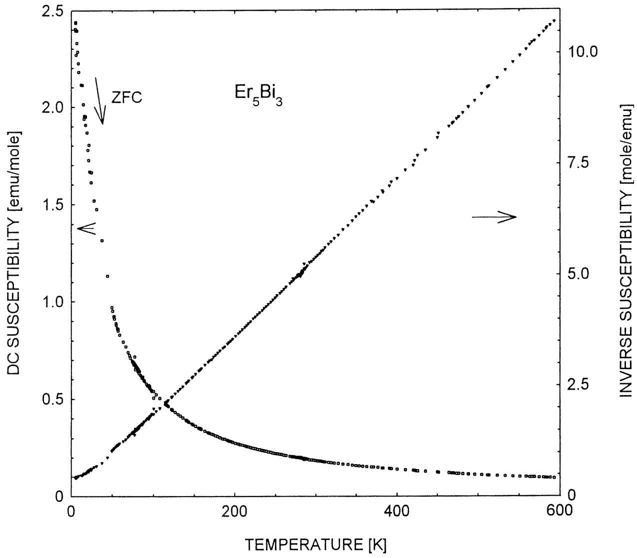

Fig. 10. Temperature dependence of magnetic susceptibility for Er_5Bi_3, zero field cooled.

For Tb_5Bi_3 the DC susceptibility shows first anomaly at about 150 K when the temperature decreases. This anomaly is however not reflected in the AC susceptibility (Fig. 11) and might be related to a slightly pronounced minimum in the resistivity (Fig. 12). The next transition at

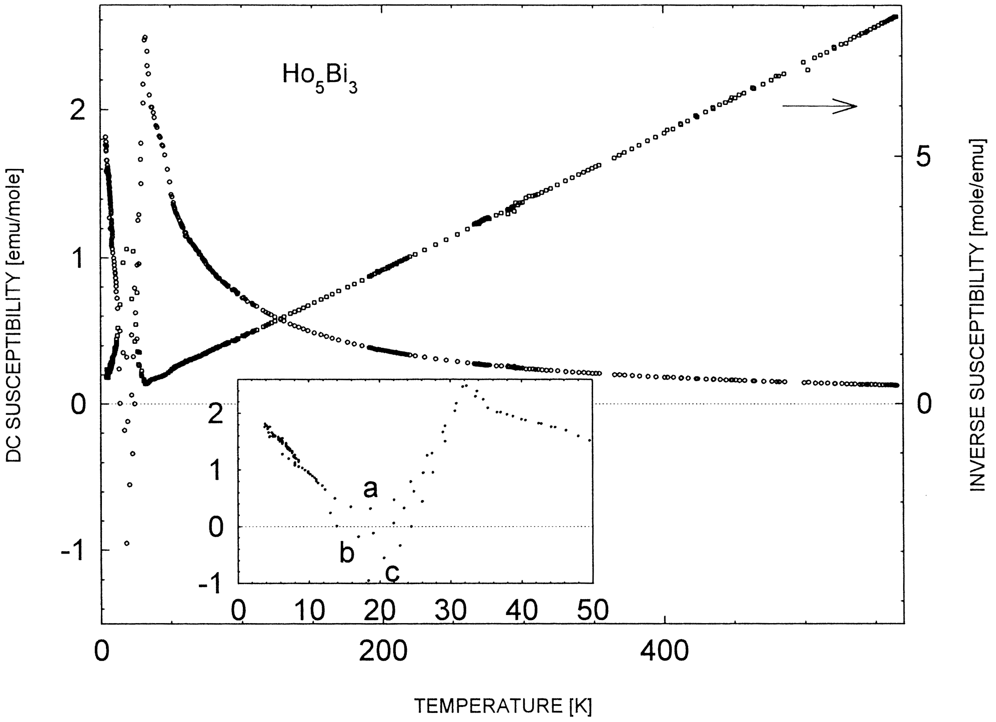

Fig. 9. Temperature dependence of magnetic susceptibility for Ho_5Bi_3. FC means cooling in the field of 674 Oe. ZFC, zero field cooling. The inset shows the region of magnetic transition where the curves were obtained at: (a) 900 Oe, ZFC; (b) 674 Oe, ZFC; (c) 674 Oe, FC.

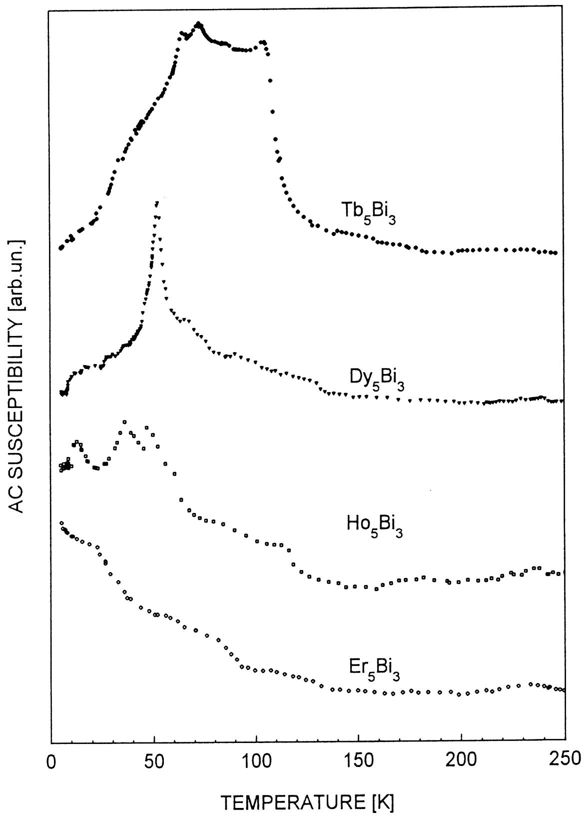

Fig. 11. AC magnetic susceptibility vs. temperature for: Tb_5Bi_3, Dy_5Bi_3, Ho_5Bi_3 and Er_5Bi_3.

about 110 K leads to a pronounced peak in the AC susceptibility. Only the transition at about 70 K is visible in the results from all used techniques. Generally, Tb_5Bi_3 exhibits a very high value of resistivity and unusual temperature dependence, which is metallic only for the temperature range 220–300 K and below 70 K. Since the abrupt change of $d\rho/dT$ at 220 K is not due to a magnetic transition, it may be related to a reversible change of crystal structure. This has to be verified with other techniques. The large thermomagnetic effect below 60 K indicates to a freezing like character of the transition, which agrees with a strong decrease of the AC susceptibility below the peak at 60 K. Frustration of magnetic interactions may be caused by the complex crystal structure where four in-equivalent RE sublattices can be found. In a ordered structure of the Y_5Bi_3-type the minimal distance between rare earth atoms is about 3.3 Å, but there is a quasi-continuous distribution of the shortest interatomic R-R distances between various positions, in the range of 3.3–4.39 Å [9]. Moreover, the analysis of the Y_5Bi_3 structure performed by Wang et al. [9] shows that Y atoms form a kind of trigonal prisms which may be a source of frustrated magnetic interactions between R atoms. Thus due to crystallographic structure there is probably a balance between the ferro-and antiferromagnetic interactions through any kind of indirect exchange, e.g. the RKKY one. An additional factor is a rare earth one–ion anisotropy. In the case of Tb_5Bi_3 cooling below 60 K at a relatively small magnetic field of 850 Oe is enough to introduce at least partial ferromagnetic order. The magnetisation dependence on magnetic field in a low field range has also a ferromagnetic character (Fig. 13).

A very large thermomagnetic effect was observed in Dy_5Bi_3 below 50 K. The susceptibility at 4.2 K differs by one order of magnitude between the zero field one and the one cooled in the field of 570 Oe. The freezing character of the transition is confirmed by the presence of a sharp peak in the AC susceptibility (Fig. 11). The transition is manifested in resistivity as a small step (Fig. 12). The most striking feature of the resisitivity run is however its constant value over a broad temperature range 50–300 K.

For Ho_5Bi_3 an unusual negative magnetisation appears in a narrow temperature range 20–30 K (Fig. 9). The negative magnetisation depends on magnetic field and on the way of cooling – with or without magnetic field as it is

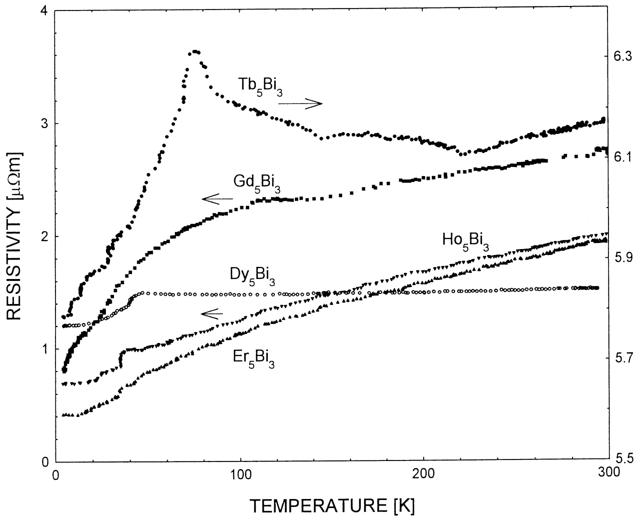

Fig. 12. Electrical resistivity for: Gd_5Bi_3, Tb_5Bi_3, Dy_5Bi_3, Ho_5Bi_3 and Er_5Bi_3.

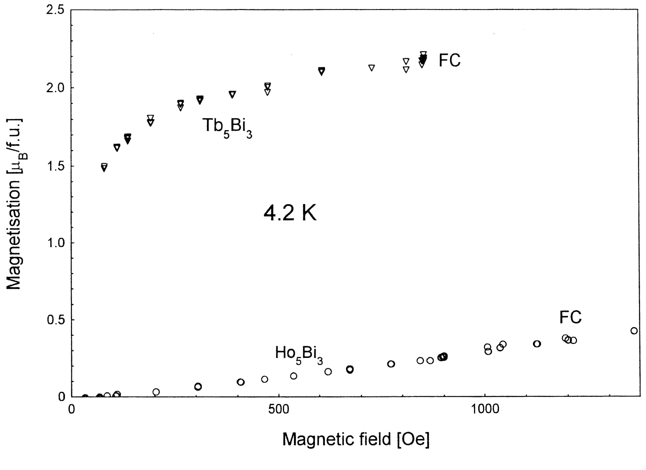

Fig. 13. Magnetisation vs. magnetic field for Tb_5Bi_3 and Ho_5Bi_3, in the low field range.

shown in the inset to the Fig. 9. The effect was checked with a different sample, which had a more spherical shape but a demagnetisation factor does not seem to influence the unusual behaviour since both samples have shown the same behaviour. This excludes also the influence of a possible texture structure of the annealed samples. A possible explanation of the observed effects is based on ordering of various Ho sublattices at various temperatures. The low external field causes that the anisotropy energy plays an important role. The peak at 32 K may be related to the appearance of an antiferromagnetic order of two or more Ho sublattices. The susceptibility of the antiferromagnetic phase decreases below T_N and a ferromagnetic interaction, which may involve only a part of Ho moments becomes more important. At the relatively low external field the anisotropy may lead the observed negative magnetisation. The susceptibility was measured using a magnetic balance and the field was switched on and off for each temperature. The effect is thus not due to an accidental alignment of magnetic domains. The field dependence of magnetisation at 4.2 K, which is presented in Fig. 13, shows a linear behaviour and the line crosses the magnetisation axis at the negative side. This indicates that also at 4.2 K, at the lowest field, a small negative magnetisation is still present. The alternating field of very low amplitude, as in the AC measurements, is not able to establish the state of negative magnetisation as it is visible in Fig. 11. First peak at 45 K corresponds to a slightly pronounced feature, which is visible also in the DC susceptibility. Then the AC susceptibility shows a peak at 35 K, which is followed by a decrease and the next peak at about 8 K. The DC run reveals a constant increase at lowest temperatures so the origin of the last peak is not clear. The resistivity shows one step-like transition at 35 K, which corresponds to the main peak in the DC susceptibility, and a slightly pronounced step at 25 K.

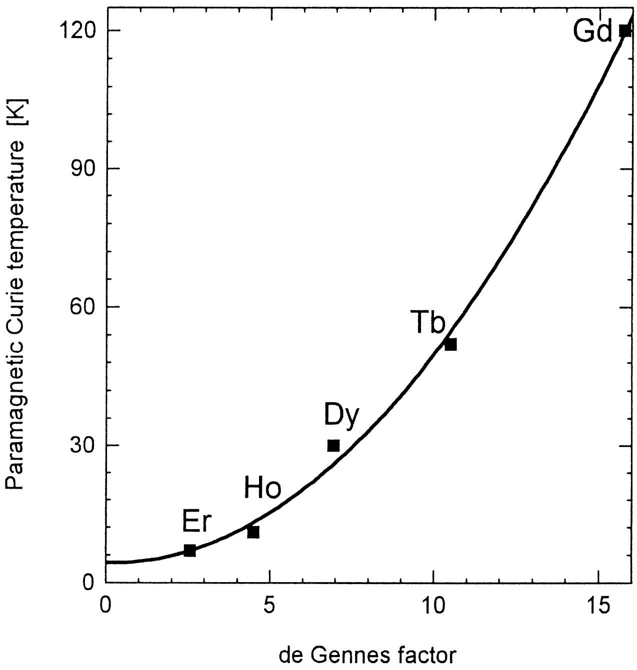

Fig. 14. Paramagnetic Curie temperature vs. de Gennes factor $(g_{J-1})^2 J(J+1)$ for R_5Bi_3. Solid line represents the parabolic approximation.

Er_5Bi_3 does not order magnetically down to 4.2 K (Figs. 10 and 11). The temperature dependence of resistivity is similar to that of the Ho compound (Fig. 13).

The magnetic properties of R_5Bi_3 compounds exhibit several features which are characteristic for all of them but in each case the ordering takes another form. The average interaction represented by the paramagnetic Curie temperature can be compared to the de Gennes factor, to check if the RKKY model is applicable. Fig. 13 shows that the relation is not linear and a parabolic function describes the experimental dependence. The photoemision measurements, which will be described in a separate paper, show that R_5Bi_3 compounds have a relatively low density of states at the Fermi level, similarly to Gd_5Bi_3. The magnetic interaction is then probably governed by the 5d electrons, which are also involved in chemical bonding. This may be one of the reasons for a non-linear θ_p dependence on the de Gennes factor (Fig. 14).

4. Conclusion

A variety of magnetic phenomena have been found in the group R_5Bi_3 compounds. The paramagnetic Curie temperature is positive for all compounds but the ordering is not simple ferromagnetic. Strong thermomagnetic effects have been observed and freezing of magnetic moments occur at low temperatures for Tb_5Bi_3 and Dy_5Bi_3. The observed effects may be related to the crystal structure which contains four inequivalent R positions in the unit cell. The alignment of the R atoms in trigonal prisms may be a reason for the frustrated magnetic interactions. Electrical resistivity depends on which R is in the compound and shows an unusual behaviour for Tb_5Bi_3. Similarly to Gd_4Bi_3, Tb_4Bi_3 orders ferromagnetically at relatively high temperature, i.e. 190 K.

Acknowledgements

We wish to thank J. Kubacki for the assistance in the AC susceptibility measurements and J. Kapusta for performing the X-ray diffraction measurements.

References

[1] H. Yamada, T. Fukawa, T. Muro, Y. Tanaka, S. Imada, S. Suga, D.X. Li, T. Suzuki, J. Phys. Soc. Jpn. 65 (1996) 1000.

[2] D.X. Li, Y. Haga, H. Shida, T. Suzuki, Y.S. Kwon, G. Kido, J. Phys.: Condens. Matt. 9 (1997) 10777.

[3] D.X. Li, Y. Haga, H. Shida, T. Suzuki, Y.S. Kwon, Phys. Rev. B 54 (1996) 10483.

[4] J. Szade, M. Drzyzga, J. Alloys Comp. 299 (2000) 72–78.

[5] M.N. Abdusalyamova, A.G. Chuiko, E.I. Shishkin, O.I. Rachmatov, J. Alloys Comp. 240 (1996) 272.

[6] W.D. Abulhajev, Metally 2 (1993) 196.

[7] K. Yoshihara, J.B. Taylor, L.D. Calvert, J.G. Despault, J. Less-Common Met. 41 (1975) 329.

[8] E. Talik, J. Szade, J. Heimann, A. Winiarska, A. Winiarski, A. Chelkowski, J. Less-Common Met. 138 (1988) 129.

[9] Yu Wang, E.J. Gabe, L.D. Calvert, J.B. Taylor, Acta Cryst. B32 (1976) 1440.